



HAL
open science

Equivalent continuous dynamic model of renewable energy systems

Benoît Robyns, Yann Pankow, Ludovic Leclercq, Bruno François

► **To cite this version:**

Benoît Robyns, Yann Pankow, Ludovic Leclercq, Bruno François. Equivalent continuous dynamic model of renewable energy systems. 7th International conference on modelling and simulation of electric machines, converters and systems: ELECTRIMACS, Aug 2002, montréal, Canada. hal-03706405

HAL Id: hal-03706405

<https://hal.science/hal-03706405>

Submitted on 27 Jun 2022

HAL is a multi-disciplinary open access archive for the deposit and dissemination of scientific research documents, whether they are published or not. The documents may come from teaching and research institutions in France or abroad, or from public or private research centers.

L'archive ouverte pluridisciplinaire **HAL**, est destinée au dépôt et à la diffusion de documents scientifiques de niveau recherche, publiés ou non, émanant des établissements d'enseignement et de recherche français ou étrangers, des laboratoires publics ou privés.

Equivalent continuous dynamic model of renewable energy systems

Benoît Robyns¹, *Member, IEEE*, Yann Pankow¹, Ludovic Leclercq¹, Bruno François², *Member, IEEE*

Abstract-- An equivalent continuous dynamic model of a renewable generating system is proposed in this paper. The models of a variable speed wind generator and of a solar generating system are particularly detailed. It is shown that these models are interesting for analyzing the dynamic behavior of the system and for designing the control strategy. The proposed global model is simulated with the help of Matlab-Simulink™, by considering a 4.5 kW wind generator and a 3.6 kW solar generator. This hybrid system is connected to a distribution network which is simulated with the help of the Power System Blockset™ (PSB) toolbox.

Index Terms-- equivalent continuous model, distribution network, photovoltaic generator, wind generator.

I. INTRODUCTION

The interest in the utilization of renewable energy increases because people feel much concerned by the environment problems. Among the renewable energy, photovoltaic (PV) panels and wind generators (WG) are now widely used [1,2]. The use of power converters enable the optimization of the energy capture from the sun and the wind. Moreover, a DC bus link allows also to combine various generators and to improve the global control of the power transfer.

The power electronic converters are by nature discrete event systems [3,4], whereas the generator and the AC grid are continuous systems. For the analysis of the dynamical behavior of the generators and for the design of the different controllers, it is worthy to define an equivalent continuous model of the global system including the power converters [4,5].

The aim of this paper is to propose equivalent continuous models of renewable energy systems. These models take into account the useful components of currents and voltages in the generating and storage systems, the DC bus and the network. These models are interesting for the following reasons:

- They are well suited for numerical integration since it is no more necessary to use an integration step in the numerical simulations which is much smaller than the converters working cycle (which depends on the switching frequency of the semi-conductors constituting the power converters). The

simulation times remain then short, which is interesting as it is often necessary to consider variations of renewable energy generators during several minutes;

- They allow simulating the global dynamical behavior of generating and storage systems, including the dynamics of the DC bus;

- They allow designing the different controllers included in the system, and particularly the DC voltage controller;

- It is easy to add in the model some complementary elements connected to the DC bus like different generators (wind generator, photovoltaic panel, battery,...), storage systems (battery, flywheel energy storage system,...) or dissipating systems without increasing the simulation computation time too much.

However, it must be noted that this equivalent model is not able to predict the voltage and current harmonics because the switching frequency is not taken into account.

An equivalent continuous dynamic model of a variable speed wind generator has been developed in [6,7]. To show the interest of the proposed method, an equivalent continuous model of a hybrid wind-photovoltaic generating system is proposed in this paper.

The proposed global model can easily be simulated with the help of a software like Matlab-Simulink™. Simulations are carried out by considering a 4.5 kW wind generator and a 3.6 kW solar generator. This hybrid generator is connected to a distribution network which is simulated with the help of the Power System Blockset™ (PSB) toolbox.

II. SYSTEM MODELING

A. Scheme of the system

Figure 1 shows the scheme of the hybrid wind-photovoltaic generating system considered in this paper. The WG is based on a squirrel cage induction machine associated to two PWM voltage source converter. The PV panels are connected to the DC bus via a boost chopper. The connection to the AC grid includes inductances to reduce the current ripples and usually a transformer.

B. Equivalent continuous model of the converters

The generators and the AC grid are continuous systems. On the other hand, the power converters are by nature discrete event systems. To obtain a global equivalent continuous model, the power converter can be reduced to simple gains between the reference waves and the a.c. outputs of the converters. But these gains depend on the DC voltage U which

Laboratoire d'Electrotechnique et d'Electronique de Puissance de Lille (L2EP)

¹ Ecole des Hautes Etudes Industrielles (HEI), 13, rue de Toul, F-59046 Lille Cedex, France, e-mail : benoit.robyns@hei.fr

² Ecole Centrale de Lille, Cité Scientifique, BP48, 59651 Villeneuve d'Ascq Cedex, France

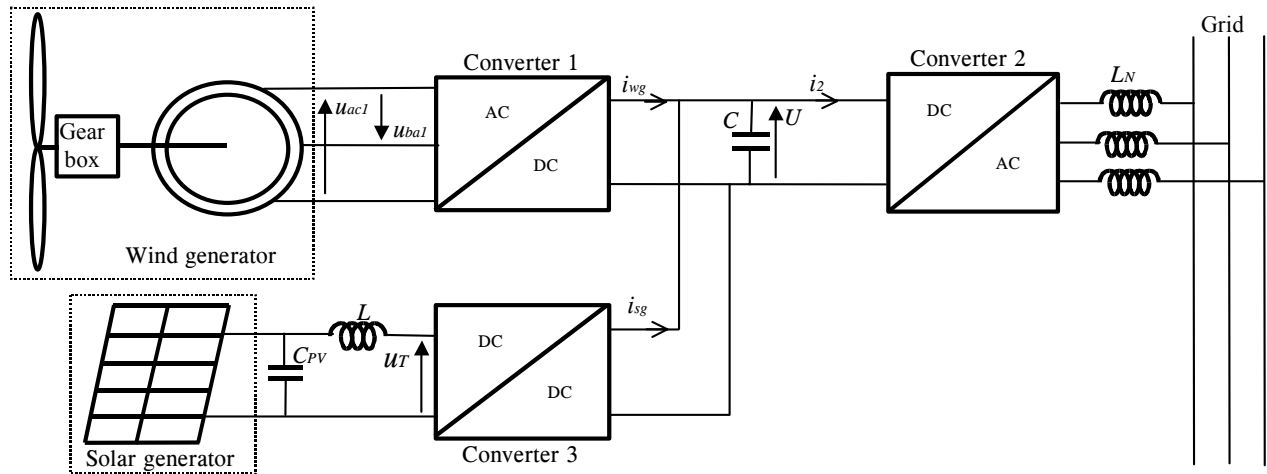


Fig. 1. Hybrid wind-photovoltaic generating system.

varies in function of the power exchanged between the generators and the network. These exchanges depend on the control strategy and on the state of the continuous systems. These interactions must be taken into account in the equivalent continuous model to analyze the dynamical behavior of the global system.

1) Inverter modeling

This study is carried out under the following assumptions:

- switches are ideal,
- they commute instantaneously and
- they are considered as short circuits in ON state and as open circuit in OFF state.

We consider that the switch in row r and column c is closed if we apply $T_{rc_1}=1$ and open if $T_{rc_1}=0$ (fig 2).

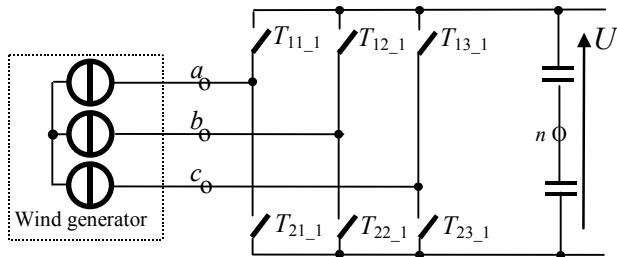


Fig. 2. Electrical diagram of the converter 1

To fulfill the fundamental laws of interconnection of sources (current sources cannot be opened and voltage sources can not be short circuited), ideal switches in a same commutation vertical circuit are in complementary states;

$$T_{1c_1} = \bar{T}_{2c_1} \quad (1)$$

In order to satisfy this constraint, a connection controller is used and, moreover, creates necessary dead times and compensates the dc-link voltage ripples from a two-level variables d_{c_1} . These bipolar control signals are obtained by comparing a control signals u_{win1} ($i \in \{a,b,c\}$) and a triangular signal ζ (fig.3). If $u_{win1} > \zeta$ then $d_{c_1} = 1$, otherwise $d_{c_1} = -1$

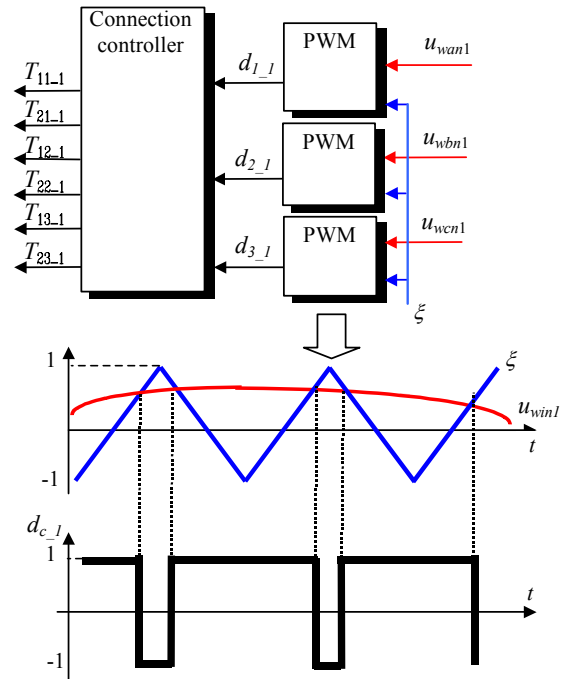


Fig. 3. Classical PWM method: comparison between a reference wave u_{win1} and a modulation wave ξ .

By introducing a mid-point, modulated voltages are easily expressed as:

$$u_{an1} = d_{1_1} \cdot \frac{U}{2} \quad (2a) \quad u_{bn1} = d_{2_1} \cdot \frac{U}{2} \quad (2b)$$

$$u_{cn1} = d_{3_1} \cdot \frac{U}{2} \quad (2c)$$

And phase to phase voltages are:

$$u_{ac1} = (u_{an1} - u_{cn1}) \quad (3a) \quad u_{ba1} = (u_{bn1} - u_{an1}) \quad (3b)$$

For a better understanding of the system, an averaged modeling of this switching power converter is necessary since the effects of high-harmonics introduced by modulators are not studied. Therefore, if the modulation frequency of the carrier signal (ζ) is much higher than the frequency domain of control signals, it can be shown that the useful components of u_{ac1} and u_{ba1} (fig. 1) are approximated by [4,5]:

$$u_{ac1} = \frac{U}{2}(u_{wan1} - u_{wcn1}) \quad (4) \quad u_{ba1} = \frac{U}{2}(u_{wbn1} - u_{wan1}) \quad (5)$$

The line voltages are then related to the control signals as follows:

$$\begin{bmatrix} u_{an1} \\ u_{bn1} \\ u_{cn1} \end{bmatrix} = \frac{U}{2} \begin{bmatrix} u_{wan1} \\ u_{wbn1} \\ u_{wcn1} \end{bmatrix} \quad (6)$$

Fig. 4 shows the equivalent electrical diagram of the converter 1.

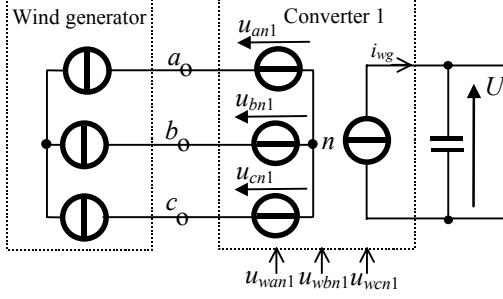


Fig. 4: Equivalent electrical diagram of the converter 1

As the model of the induction machine will be developed into the d-q coordinate frame the Park transformation (7) is applied to both members of (6).

$$[P] = \sqrt{\frac{2}{3}} \begin{bmatrix} \cos \theta & \cos\left(\theta - \frac{2\pi}{3}\right) & \cos\left(\theta - \frac{4\pi}{3}\right) \\ -\sin \theta & -\sin\left(\theta - \frac{2\pi}{3}\right) & -\sin\left(\theta - \frac{4\pi}{3}\right) \\ \frac{1}{\sqrt{2}} & \frac{1}{\sqrt{2}} & \frac{1}{\sqrt{2}} \end{bmatrix} \quad (7)$$

One gets then:

$$\begin{bmatrix} u_{sd1} \\ u_{sq1} \end{bmatrix} = \frac{U}{2} \begin{bmatrix} u_{wd1} \\ u_{wq1} \end{bmatrix} \quad (8)$$

It may be noticed that the reference waves u_{wij} are per unit values. Fig. 5 shows the equivalent electrical diagram of the converter 1 in d,q frame.

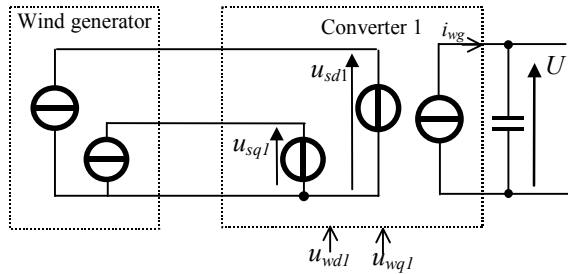


Fig. 5: Equivalent electrical diagram of the converter 1 in the d,q frame

For converter 2, one gets similar relations between the reference voltages (u_{wd2} , u_{wq2}) and the d-q components of the actual voltages:

$$\begin{bmatrix} u_{d2} \\ u_{q2} \end{bmatrix} = \frac{U}{2} \begin{bmatrix} u_{wd2} \\ u_{wq2} \end{bmatrix} \quad (9)$$

The evolution of the DC voltage U is linked to the current i in the capacitor C . This current depends on the currents at the DC side of each converter. They can be related to the d-q

components of the AC currents by equaling for each converter the average value of the power on the DC side with the active power on the AC side [4,5]. For converter 1, one gets:

$$U i_{wg} = u_{an1} i_{a1} + u_{bn1} i_{b1} + u_{cn1} i_{c1} \quad (10)$$

By taking into account the relation (6), (10) becomes:

$$i_{wg} = \frac{1}{2} (u_{wan1} i_{a1} + u_{wbn1} i_{b1} + u_{wcn1} i_{c1}) \quad (11)$$

By applying an inverse Park transformation to the three reference waves and to the three AC currents, (11) can be rewritten as follows:

$$i_{wg} = \frac{1}{2} (u_{wd1} i_{sd1} + u_{wq1} i_{sq1}) \quad (12)$$

For converter 2, a similar relation is obtained:

$$i_2 = \frac{1}{2} (u_{wd2} i_{d2} + u_{wq2} i_{q2}) \quad (13)$$

2) Chopper modeling

Converter 3 is a voltage boost chopper (fig.6). As for the inverters, the useful components of the transistor voltage u_T can be related to the DC bus voltage with the help of a reference wave u_w :

$$u_T = u_w U \quad (14)$$

The current i_{sg} generated by the PV generator on the DC bus can easily be calculated if the chopper losses are neglected; the powers at each side of the converter are then equals.

$$i_L u_T = U i_{sg} \quad (15)$$

By introducing (14) in (15), one gets

$$i_{sg} = i_L u_w \quad (16)$$

As the boost chopper generates only positive voltage, reference wave u_w is related to the duty cycle α by the following relation [4,5]:

$$u_w = (1 - \alpha) \quad (17)$$

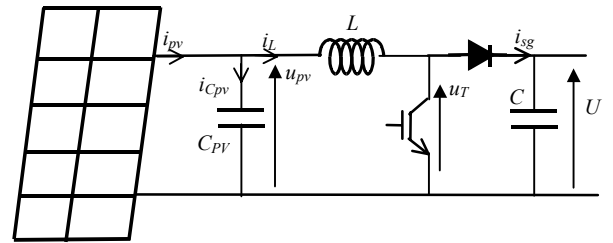


Fig. 6: Photovoltaic generating system.

3) DC bus modeling

The evolution of the DC voltage U is then determined by the following relation:

$$\frac{dU}{dt} = \frac{1}{C} (i_2 - i_{wg} - i_{sg}) \quad (18)$$

C. Induction machine and wind turbine models

By taking into account the relation (9) between the stator voltages u_{sd1} , u_{sq1} and the reference voltages, the electrical

equations of the induction machine are, in a generalized two axes reference frame:

$$\frac{di_{sd1}}{dt} = -\frac{R_s}{\sigma L_s} i_{sd1} + \omega_1 i_{sq1} - \frac{M}{\sigma L_s L_r} \frac{d\Psi_{rd1}}{dt} + \omega_1 \frac{M}{\sigma L_s L_r} \Psi_{rq1} + \frac{1}{\sigma L_s} u_{wd1} \frac{U}{2} \quad (19a)$$

$$\frac{di_{sq1}}{dt} = -\omega_1 i_{sd1} - \frac{R_s}{\sigma L_s} i_{sq1} - \omega_1 \frac{M}{\sigma L_s L_r} \Psi_{rd1} - \frac{M}{\sigma L_s L_r} \frac{d\Psi_{rq1}}{dt} + \frac{1}{\sigma L_s} u_{wq1} \frac{U}{2} \quad (19b)$$

$$\frac{d\Psi_{rd1}}{dt} = -\frac{R_r}{L_r} \Psi_{rd1} + (\omega_1 - P\omega_m) \Psi_{rq1} + \frac{MR_r}{L_r} i_{sd1} \quad (19c)$$

$$\frac{d\Psi_{rq1}}{dt} = -(\omega_1 - P\omega_m) \Psi_{rd1} - \frac{R_r}{L_r} \Psi_{rq1} + \frac{MR_r}{L_r} i_{sq1} \quad (19d)$$

$$\frac{d\omega_m}{dt} = \frac{1}{J} \left(P \frac{M}{L_r} (i_{sq1} \Psi_{rd1} - i_{sd1} \Psi_{rq1}) - K_v \omega_m - T_m \right) \quad (19e)$$

In these equations, $\Psi_{rd1}, \Psi_{rq1}, i_{sd1}, i_{sq1}$ are the rotor fluxes and the stator currents, with respect to an arbitrary d, q axes frame; M is the mutual inductance between the stator and the rotor d, q equivalent windings; L_s and L_r are the inductances of the stator and of the rotor d, q equivalent windings. $L_s = M + l_{so}$ and $L_r = M + l_{ro}$ where l_{so} and l_{ro} are the leakage inductances of the stator and the rotor windings. R_s and R_r are the resistances of the stator and rotor d, q windings; ω_1 is the angular speed of the d, q reference frame with respect to the stator and ω_m is the mechanical speed; P the number of pairs of poles. The parameter $\sigma = 1 - M^2 / (L_s L_r)$ is the dispersion coefficient of the machine. K_v is the viscous friction coefficient, J is the inertia coefficient and T_m is the mechanical torque.

A simplified wind turbine model is used with mean wind speed v as input, as the blades are assumed to be infinitely rigid. If the mechanical gear is assumed without loss and the gear ratio equal G , the mechanical torque T_m of the induction generator is given by:

$$T_m = \frac{1}{2} C_p \rho S \frac{v^3}{G \omega_t} \quad (20)$$

Where ρ is the air density, S is the swept area of the rotor and C_p is the power efficiency coefficient which is a function of tip speed ratio k and blade pitch angle. The tip speed ratio is defined as the ratio of wind turbine rotor speed ω_t to wind speed [1,7]:

$$k = \frac{\omega_t R}{v} \quad (21)$$

R is the radius of the turbine.

D. Photovoltaic generating system model

From fig. 6, by taking into account relation (14), the

following equations can be deduced:

$$\frac{du_{pv}}{dt} = \frac{1}{C_{pv}} (i_{pv} - i_L) \quad (22a)$$

$$\frac{di_L}{dt} = \frac{1}{L} (u_{pv} - u_w U) \quad (22b)$$

E. Network model

To test both models of generators, a distribution network has been developed with the Power System Blockset™ toolbox of Matlab-Simulink™. This network is shown in fig. 7.

The distribution network is composed of a Δ , y transformer, π -line models with different length and three identical loads. The hybrid generator model is connected at the node 3. To permit the exchange of informations between simulink models and PSB models, an interface is necessary. This interface is described in fig. 8.

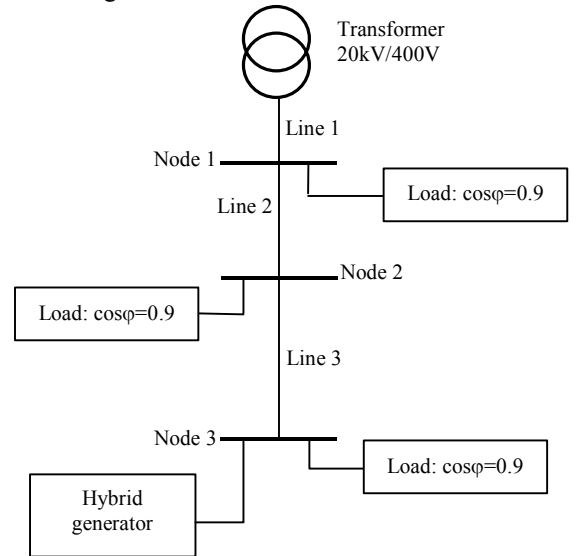


Fig 7. Distribution network model.

III. CONTROL STRATEGY

A. Control of the induction machine

To control the induction generator, a fuzzy logic based multimodel field oriented control is chosen [8,9]. This control strategy is very few sensitive to parameter uncertainties and allows to optimize the flux and the torque control. Moreover, this control algorithm can be treated with a sampling period of several hundreds of μs .

The speed of the induction generator is controlled. The reference speed is deduced from the wind speed by (21), by taking into account the gear ratio. k is chosen to optimize the power efficiency coefficient C_p [6,7].

B. Control of the photovoltaic system

The aim of the PV control strategy is to adjust the voltage u_{pv} to have the maximum power extraction.

This is obtained with the help of a Maximum Power Point Tracking (MPPT) technique [1,2]. From the state equations (22), it can be deduced that two controllers must be considered to control respectively the voltage u_{pv} and the current i_L which

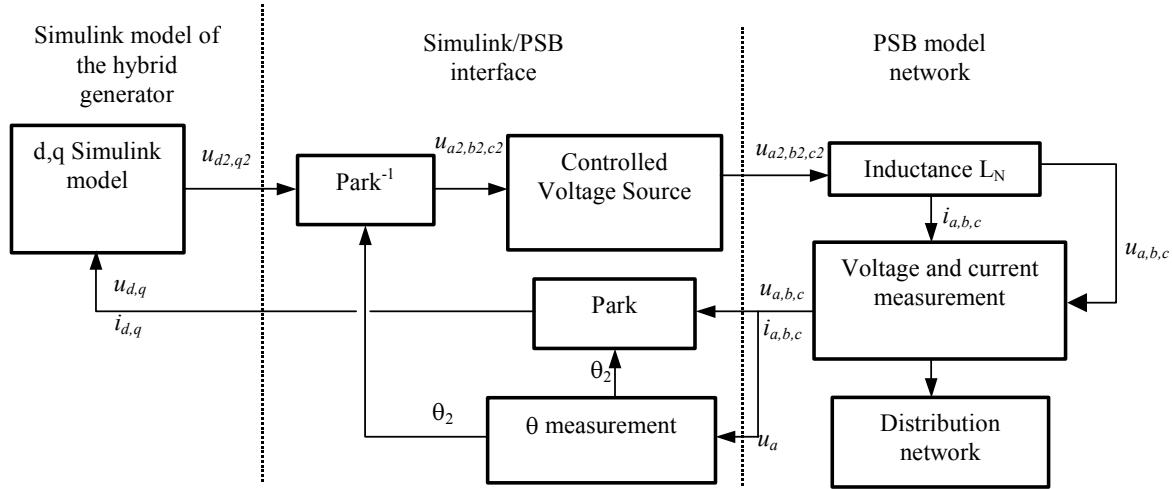


Fig 8. Interface between the hybrid generator model and the distribution network.

are two state variables. By taking into account the MPPT technique, the control strategy shown in figure 9 is naturally deduced from the proposed model.

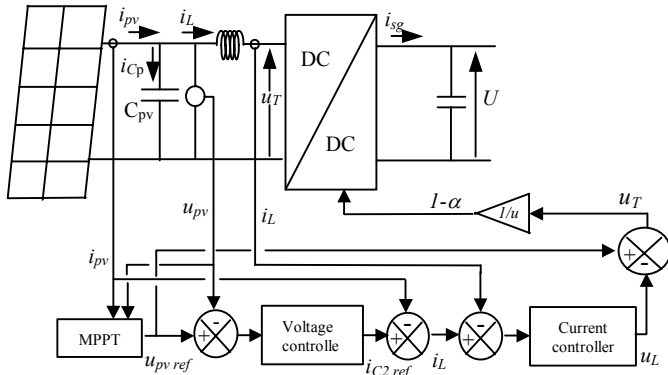


Fig. 9. Control of the photovoltaic system.

C. Control of the power exchanged with the AC grid

The considered control strategy of the active and reactive power exchanged with the AC grid is presented in [10,11]. Classically, the active power reference value is determined by the continuous voltage controller. This power reference depends in fact on the active power consumed or generated by the induction machine and generated by the PV modules, which can be estimated from (12) and (16) as follows:

$$P_{ref}^i = U_{ref} i_{wg} + U_{ref} i_{sg} \quad (23)$$

U_{ref} is the DC voltage reference value. Fig. 10 shows the continuous voltage control and the active power reference value determination taking into account (23). The DC voltage control compensates the converter losses which are neglected in (23).

The setting of the reactive power reference value may be equal to zero or to a value which allows to compensate reactive power in the AC grid.

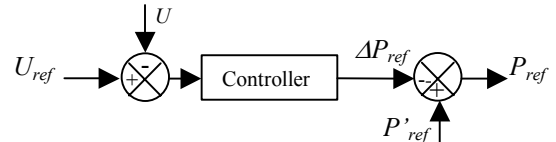


Fig. 10. DC voltage control and active power reference value generation.

IV. SIMULATIONS

The model of the system shown in figure 1 is described by 8 state equations without taking account the network: (18), (19) and (22).

The hybrid generator is connected at the node 3 (figure 7). The network is composed of three loads of 20 KW with a $\cos\phi=0.9$. The length of a line is 150 m, the distance between the hybrid generator and the transformer is 450m. Aluminium cable stich is chosen to connect all the loads.

Figure 11 shows the wind speed variation about 12 m/s considered in the simulation. The wind generator is controlled in order to capture the maximum wind energy. The illuminance during this time is random, as shown the figure 12, varies up to 200 W/m² to 1000 W/m². The panel model considered has an efficiency of 15%.

Figure 13 shows the DC bus voltage. The reference value of 700V is well followed because of the feedforward action introduced in the DC bus voltage control. Figure 14 shows the controlled current i_L in the PV generator. The variations of this current is close to the variation of the illuminance.

The active power exchanged between the network and the hybrid generator is shown in figure 15. The power fluctuations induce variations in the RMS voltage value at the node 3 as shown in figure 16.

Figure 13 to 16 show that the equivalent continuous model allows to describe the internal behaviour of the generators, and their impact on the network where they are connected.

V. CONCLUSION

Equivalent continuous models of renewable energy systems have been proposed in this paper. To show the interest of the proposed method, an equivalent continuous model of a hybrid

wind-photovoltaic generating system has been particularly developed. This model is interesting for analyzing the dynamic behavior of the whole system and for designing the control strategy. The proposed global model can easily be simulated with the help a software like Matlab-Simulink^{TD}. Simulations have been carried out by considering a 4.5 kW wind generator and a 3.6 kW solar generator. This hybrid generator has been connected to a distribution network simulated with the help of the Power System BlocksetTM (PSB) toolbox.

VI. REFERENCES

- [1] R. Mukand Patel, "Wind and solar power systems", CRC Press, 1999.
- [2] F. Giraud, Z.M. Salameh, "Steady-state performance of a grid connected rooftop Hybrid wind-photovoltaic power system with battery storage", *IEEE Trans on Energy Conversion*, Vol 16, March 2001, pp1-7.
- [3] J.P.Hautier, J.P.Caron, "Convertisseurs statiques, méthodologie causale de modélisation et de commande", Editions Tecnip, 1999.
- [4] F. Labrique, H. Buyse, G. Séguier, R. Bausière, "Les convertisseurs de l'électronique de puissance, Commande et comportement dynamique", Tome 5, Technique et Documentation - Lavoisier, 1998.
- [5] H. Buyse, D. Grenier, F. Labrique, S. Gusia, "Dynamic modelling of power electronic converters using a describing function like approach", *Proceedings of Electrimacs'99*, Lisbon, September 1999, pp. 1-7-1-14.
- [6] B. Robyns, M. Nasser, F. Berthereau, F. Labrique, "Equivalent continuous dynamic model of a variable speed wind generator", *Electromotion*, vol. 8, n°4, 2001, pp. 202-208.
- [7] B. Robyns, M. Nasser, "Modélisation et simulation d'une éolienne à vitesse variable basée sur une génératrice asynchrone à cage", *Actes du colloque Electrotechnique du Futur, EF'01*, Nancy, november 2001, pp.77-82.
- [8] F. Berthereau, B. Robyns, J.P. Hautier, "A fuzzy logic based multimodel F.O.C of an induction generator for wind power systems" *Electromotion 2001*, Bologne, June 2001, pp 571-576.
- [9] F. Berthereau, B. Robyns, J.P. Hautier, H.Buyse, "Commande vectorielle multimodèle de la machine asynchrone avec superviseur à logique floue", *Revue Internationale de Génie Electrique*, volume 4, 2001, n° 3-4, pp 343-365.
- [10] B. Robyns, M. Esselin, "Power control of an inverter-transformer association in a wind generator", *Electromotion*, vol 6, n°1-2, 1999, pp3-7.
- [11] M. Esselin, B. Robyns, F. Berthereau, J.P Hautier, "Resonant controller based power control of an inverter transformer association in a wind generator", *Electromotion*, vol 7, n°4, 2000, pp 185-190.

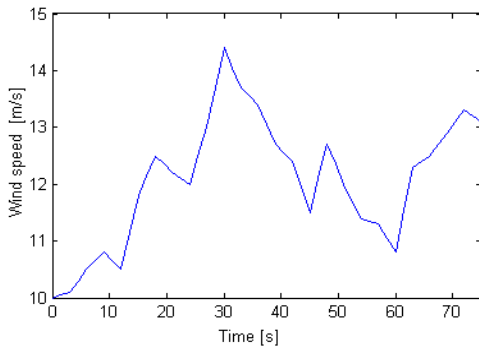


Fig. 11. Measured wind speed considered in the simulation

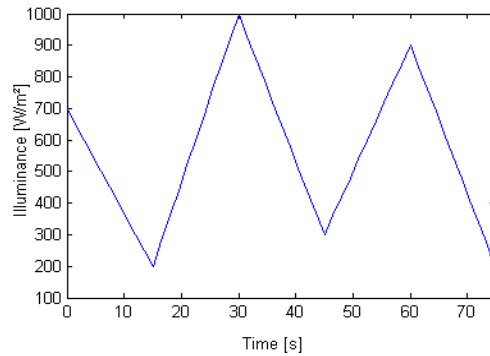


Fig. 12. Random illuminance considered in the simulation

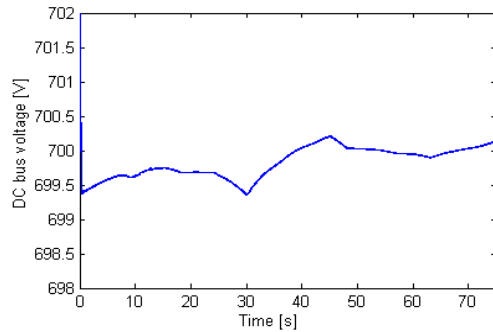


Fig. 13. DC bus voltage

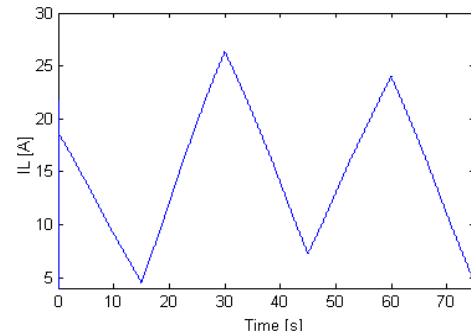


Fig. 14. Controlled current i_L in the PV generator.

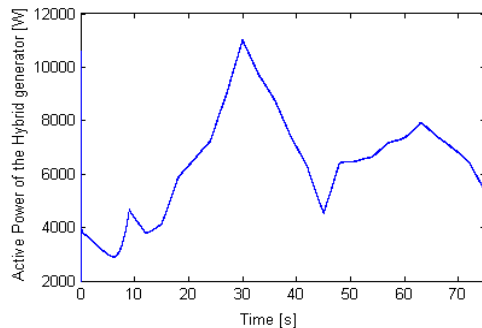


Fig. 15. Active power exchanged with the network

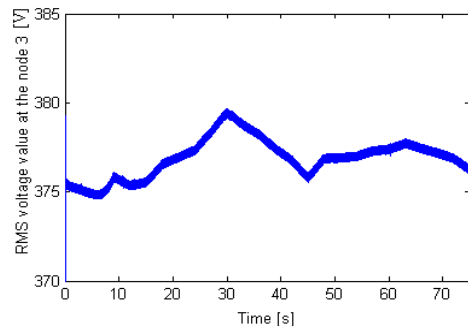


Fig. 16. RMS voltage value at the node 3